Protein Engineering vol.13 no.7 pp.491–500, 2000

Effects of pore mutations and permeant ion concentration on the spontaneous gating activity of OmpC porin

Nazhen Liu[1], Hrissi Samartzidou[2], Keun Woo Lee, James M.Briggs and Anne H.Delcour[3]

Department of Biology and Biochemistry, University of Houston, Houston, TX 77204-5513, USA

[1]Present address: Department of Neurobiology and Anatomy, University of Texas–Houston Medical School, P.O. Box 20708, Houston, TX 77225, USA

[2]Present address: Molecular Dynamics, 928 East Arques Avenue, Sunnyvale, CA 94086-4520, USA

[3]To whom correspondence should be addressed. E-mail: adelcour@uh.edu

Porins are trimers of β-barrels that form channels for ions and other hydrophilic solutes in the outer membrane of Gram-negative bacteria. The X-ray structures of OmpF and PhoE show that each monomeric pore is constricted by an extracellular loop that folds into the channel vestibule, a motif that is highly conserved among bacterial porins. Electrostatic calculations have suggested that the distribution of ionizable groups at the constriction zone (or eyelet) may establish an intrinsic transverse electrostatic field across the pore, that is perpendicular to the pore axis. In order to study the role that electrostatic interactions between pore residues may have in porin function, we used spontaneous mutants and engineered site-directed mutants that have an altered charge distribution at the eyelet and compared their electrophysiological behavior with that of wild-type OmpC. We found that some mutations lead to changes in the spontaneous gating activity of OmpC porin channels. Changes in the concentration of permeant ions also altered this activity. These results suggest that the ionic interactions that exist between charged residues at the constriction zone of porin may play a role in the transitions between the channel's closed and open states.

Keywords: channel/*Escherichia coli*/gating/mutant/OmpC porin/patch-clamp/pore mutations

Introduction

Porins are trimers of β-barrels that form channels for ions and other hydrophilic solutes in the outer membrane of Gram-negative bacteria (Nikaido, 1996). The three-dimensional structure of many bacterial porins is known at atomic resolution (Weiss *et al.*, 1991; Cowan *et al.*, 1992; Schirmer *et al.*, 1995; Pautsch and Schulz, 1998; Dutzler *et al.*, 1999). The constriction region or 'eyelet' of bacterial porin is formed in part by the wall of the β-barrel and in part by an extracellular loop folded into the channel vestibule (Figure 1). The charge distribution in this region is conserved amongst all porins of known structures and consists of negatively charged residues on the folded loop and positively charged residues in the opposite barrel wall. This conservation suggests an essential role of these residues in both the structure and function of porin channels.

It has been clearly established that the charged residues of the eyelet play a role in determining channel size. For example, spontaneous mutants in these residues were obtained in OmpC or OmpF by screening for strains that are able to grow on maltodextrins as sole carbon source in the absence of LamB, the natural transporter for these large molecules (Benson *et al.*, 1988; Misra and Benson, 1988). Since maltodextrins are too bulky to penetrate the wild-type channels, the mutants form channels with an increased pore size, as shown by an increased uptake rate of radiolabeled maltose in cells and a larger single channel conductance (Benson *et al.*, 1988; Delcour *et al.*, 1991; Lakey *et al.*, 1991).

It appears that the electrostatic configuration of the eyelet may play even a greater role than structural constraints in properties such as size exclusion, solute transport and selectivity. Calculations of the electrostatic features of OmpF and PhoE porins suggest that the distribution of the ionizable groups at the eyelet establishes an intrinsic transverse electrostatic field across the pore, that is perpendicular to the pore axis (Karshikoff *et al.*, 1994). It has been proposed that the electrostatic field may facilitate the dehydration of polar solute molecules passing through the pore (Weiss *et al.*, 1991) and may also be important for the exclusion of hydrophobic molecules and the transport of charged or polar compounds (Karshikoff *et al.*, 1994; Schulz, 1996). Recently, it has been suggested that the difference in pore size between OmpF and OmpK36 (an OmpC homolog) does not reside in structural differences but rather in the distinct electrostatic profiles close to the internal loop (Dutzler *et al.*, 1999). Comparisons between OmpF and PhoE also suggest that the electrostatic profile contributes to the ion selectivity of the porin channel (Karshikoff *et al.*, 1994) and the involvement of specific charged residues of the eyelet in determining selectivity has been demonstrated experimentally (Saint *et al.*, 1996; Bauer *et al.*, 1989).

The role of the intrinsic potential in the dynamic properties of porin channels has been more elusive. There is substantial evidence for the voltage-dependent gating of porin channels *in vitro*. When the transmembrane potential reaches a certain threshold (~150 mV), stepwise closures of single or multiple porin monomers occur owing to the transition of channels into a prolonged closed or inactivated state (Schindler and Rosenbusch, 1978; Dargent *et al.* 1986; Xu *et al.*, 1986; Lakey, 1987). These voltage-induced closures are also observed in patch-clamp experiments with reconstituted purified proteins (Berrier *et al.*, 1992, 1997) and outer membrane fractions (Delcour *et al.*, 1989b, 1991; Delcour, 1997; Samartzidou and Delcour, 1998), where a combination of fast and slow gating kinetics is detected at relatively lower transmembrane voltages (<100 mV). Characterization of OmpC (Delcour *et al.*, 1991; Lakey *et al.*, 1991), OmpF (Saint *et al.*, 1996) and PhoE (Van Gelder *et al.*, 1997) mutants revealed that the charged residues contributing to the transverse electrical field play the role of voltage sensors. It was proposed that the positive residues in the barrel are the voltage sensors in the anion-selective porins, such as PhoE, whereas the negative charges on the L3 loop

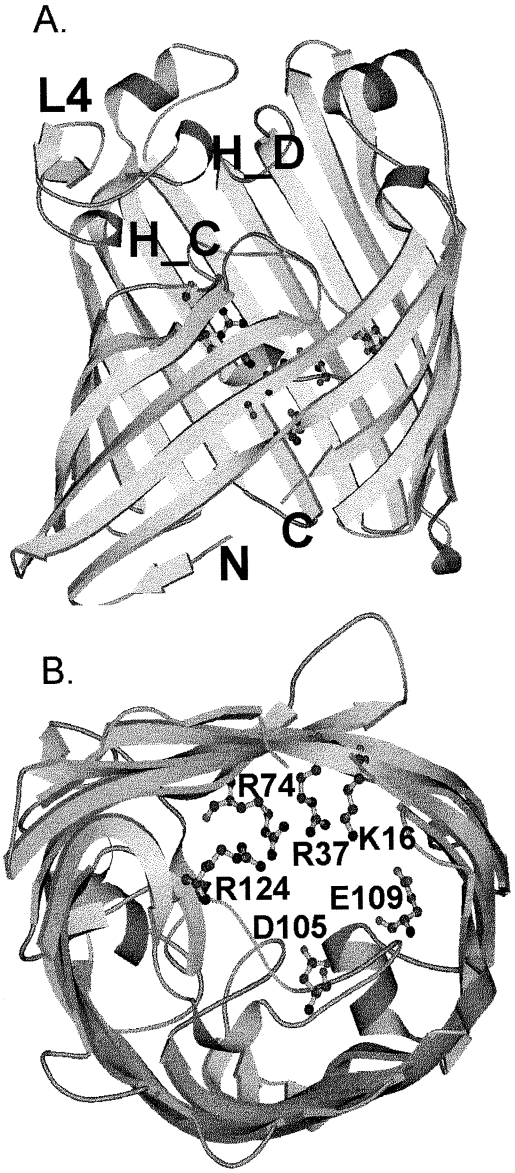

Fig. 1. Homology model of OmpC. (**A**) Side-view of a monomer, with extracellular side on top. H_C and H_D mark the small helices in the L4 region. (**B**) Cross-section of a monomer, viewed from the periplasmic side. The six mutated residues of the constriction zone are labeled. The figures were drawn with the Molscript program (Kraulis, 1991).

are responsible for voltage sensing in the cation-selective porins, such as OmpF and OmpC (Van Gelder *et al.*, 1997). This difference between the two porin types was later correlated with their opposite voltage dependence (Samartzidou and Delcour, 1998). Although the L3 loop might harbor the voltage sensors, it does not appear to undergo any major motion that is required for voltage-dependent closure. Indeed, recent experiments strongly exclude a gross movement of the L3 loop as the mechanism underlying the voltage-dependent gating, because no change in voltage sensitivity is observed when the loop is tethered to the barrel by various engineered disulfide bridges (Eppens *et al.*, 1997; Phale *et al.*, 1997; Bainbridge *et al.*, 1998).

For this reason, in the work reported here, we focused our attention not on the voltage-dependent activity, but on the spontaneous gating of channels between closed and open states. This activity is clearly observed in patch-clamp experiments, but is not typically a point of interest in studies done with planar lipid bilayers (Delcour, 1997). This spontaneous activity is, however, strongly modulated by various parameters (Delcour *et al.*, 1989b; Iyer and Delcour, 1997; Liu and Delcour, 1998b) and represents an important aspect of the dynamic properties of the channel. To understand the role of the intrinsic electrical potential in the spontaneous gating activity, we compared the electrophysiological behavior of wild-type channels with that of site-directed or spontaneous mutants that have an altered charge distribution at the eyelet. Since most of our previous studies were performed on OmpC (Delcour *et al.*, 1991; Liu *et al.*, 1997; Liu and Delcour, 1998a,b), we pursued our work with this protein. OmpC is highly homologous to other porins, such as OmpF, PhoE and OmpK36 (Mizuno *et al.*, 1983; Alberti *et al.*, 1995) and we used the structural information obtained from these porins to build a homology model and to design mutants in OmpC. Our results suggest that the ionic interactions that exist between charged residues at the constriction zone of porin may play a role in the transitions between the channel closed and open states.

Materials and methods

Sequence alignment and homology modeling of Escherichia coli OmpC

Sequence alignment was performed between *E.coli* OmpC, OmpF and PhoE (Mizuno *et al.*, 1983) and *Klebsellia pneumoniae* OmpK36 (Alberti *et al.*, 1995). The sequence identities with *E.coli* OmpC are 60% for OmpF, 59% for PhoE and 79% for OmpK36. All sequences were obtained from the SWISS-PROT data bank. The sequence data were manipulated using the Homology modules of InsightII (Molecular Simulations). Most of the sequence of OmpC had a corresponding sequence from the three template proteins except for the stretch between residues 154 and 167, in the L4 loop. This region was refined after structure generation, since it is fairly long and without proper correspondence with the reference proteins.

The Discover module of InsightII was used for the simulation, along with the CVFF forcefield (Dauber-Osguthorpe *et al.*, 1988). The geometry of the entire protein was held fixed throughout the refinement procedure with the exception of residues 151–178. A distance-dependent dielectric constant was introduced to add some solvent effect. The short- and long-range cutoffs for the electrostatic and van der Waals interactions were 10 and 14 Å, respectively. Minimization was performed using the steepest descents algorithm for 100 steps, followed by the conjugate gradient scheme until the structure converged to within a tolerance 0.1 kcal/mol.Å. The resulting structure was used to start a molecular dynamics simulation of 200 ps after 1000 steps (1 ps) of equilibration during which a 1 fs time step was used. The time step was 1 fs for the production phase of the simulation, since the SHAKE algorithm was not used to constrain any bond lengths. Analysis of the trajectory from the production phase of the MD simulation revealed that the motion of L4 stabilized after about 50 ps. Therefore, the last conformation from the MD simulation was chosen as the final three-dimensional structure of OmpC since it appeared to be well refined. The overall secondary structural elements of OmpC are very similar to those in the other porins, yielding a β-barrel structure for the main body of the porin and a constriction zone established by the folded L3 loop.

Two small α-helices are present in L4 bewteen residues 152 and 154 and residues 172 and 174 (as in OmpK36).

The homology model of OmpC (Figure 1) was built from the template *pdb* structures of *E.coli* OmpF (1opf) and PhoE (1pho) (Cowan *et al.*, 1992) and *K.pneumoniae* OmpK36 (1osm) (Dutzler *et al.*, 1999). The three-dimensional structures were generated by Modeler (Sali and Blundell, 1993; Sali *et al.*, 1995). The root mean square deviations (r.m.s.d.s) for backbone atoms of the final homology structure of OmpC with OmpF, PhoE and OmpK36 are 1.38, 1.42 and 0.68 Å, respectively. In the pore region, the r.m.s.d.s for backbone atoms of the L3 loop are 0.78 Å between OmpC and OmpF and 0.21 Å between OmpC and OmpK36. These values are similar to the r.m.s.d. of 0.85 Å obtained for backbone atoms of the L3 loop between the X-ray structures of OmpF and OmpK36. Thus, in the pore region, the modeled structure of OmpC is highly similar to those of crystallized porins.

Dipole moment calculation

The homology modeled structure of OmpC generated as described above was used for the charge and dipole moment calculations. Previous electrostatic calculations of OmpF and PhoE porins also showed that there were many ionizable residues that had unusual net charges (Karshikoff *et al.*, 1994). Therefore, in order to obtain more realistic values of the net charges of all ionizable residues in the protein, we used an automated procedure based on an electrostatic method that takes into account solvation/desolvation, ionic strength and correlated titration behavior. The prediction ionization states are in general accord with those obtained previously (Karshikoff *et al.*, 1994). A number of acidic residues exhibit shifted ionization states and the sole His residue is predicted to be ionized at pH 7.To compare with the results of experimental studies, mutations of the wild-type OmpC structure were generated with use of the Biopolymer module of InsightII for six residues shown in Figure 1 and the structures of K16Q, K16R, R37H, R74S, R37H/R74S, D105Q, E109Q and R124Q mutants were constructed from the wild-type structure. The ionization state prediction procedure of the UHBD (University of Houston Brownian Dynamics) program was employed for the net charge predictions (Madura *et al.*, 1995; Antosiewicz *et al.*, 1996; Fogolari *et al.*, 1998). The GRASP program (Gilson and Honig, 1988; Nicholls *et al.*, 1991) was used for the dipole moment calculations from the modified partial charges generated by the ionization state predictions. All the modeling was done with monomeric protein.

Chemicals, bacterial strains and mutant construction

A kanamycin-resistant plasmid containing a cloned OmpC gene (pNLC10) was used as the template to introduce site-directed mutations into OmpC with the unique site elimination method (USE, Pharmacia) as described previously (Liu *et al.*, 1997). All mutations (K16Q, K16R, D105Q, E109Q, E109D, R124Q) were confirmed by DNA sequencing of the whole gene. The wild-type or mutated plasmid was introduced in an *E.coli* K12 strain derived from AW737 (Ingham *et al.*, 1990) and deleted for OmpC and OmpF from the chromosome, as described previously (Liu *et al.*, 1997). The R37H, R74S and R37H/R74S mutants are spontaneous chromosomal mutants, isolated by Misra and Benson (1988). The corresponding mutant strains (RAM272, RAM120, RAM359) and their isogenic parent (RAM105) were kindly provided by Dr S.Benson.

Tryptone growth medium (T-broth) contained 1% tryptone (Difco Laboratories) and 0.5% NaCl. Azolectin (phosphatidylcholine, type IIS) and isopropyl β-D-thiogalactopyranoside (IPTG) were obtained from Sigma. All other chemicals were purchased from Fisher Scientific. Enzymes used in molecular biology protocols were purchased from either Gibco or Promega. The DNA sequencing kit was obtained either from United States Biotechnology or Perkin-Elmer and the DNA purification kit from Promega or Qiagen. The determination of protein concentration was done by the bicinchoninic acid method (Pierce).

Membrane preparation and patch-clamp electrophysiology

Strains expressing wild-type or mutated OmpC were grown in T-broth to mid-log phase with 0.7 mM IPTG if required. After cells had been harvested by centrifugation, outer membrane fractions were purified by sucrose gradient centrifugation, as published (Delcour *et al.*, 1989a). Patch-clamp experiments (Hamill *et al.*, 1981) were performed on blisters induced from giant liposomes containing the reconstituted outer membrane fractions (Delcour *et al.*, 1989a; see cartoon description in Liu and Delcour, 1998a). Pipets had an initial resistance of 10 MΩ. Protein:lipid ratios of 1600–1700 typically yielded seals of 0.7–1.3 GΩ, due to the presence of multiple open porin channels in the patch. Patches were excised by air exposure. Unless noted otherwise, pipet and bath solutions were 150 mM KCl, 5 mM HEPES, 0.1 mM K-EDTA, 0.01 mM $CaCl_2$, pH 7.2. Currents were filtered at 2 kHz with a eight-pole Bessel filter (Frequency Devices) and recorded with an Axopatch-1D amplifier (Axon Instruments). Continuous recordings were made on VCR tapes. For analysis, the data were re-filtered at 1 kHz and digitized at 100 μs sampling intervals (Instrutech). Data acquisition and analysis were done with programs developed in the laboratory using Axobasic (Axon Instruments).

Identification of OmpC channels and data analysis

Although we performed our experiments on outer membrane fractions and not on purified proteins, we ascertained that the recorded activities originate from OmpC because (1) the host strain lacks chromosomal porin genes and the expression of the sole major porin, OmpC, is driven from the plasmid, (2) the channel activity is absent in a mutant lacking OmpF and OmpC and no other channel activities are observed (Delcour *et al.*, 1992) and (3) as shown in this and previous studies (Liu *et al.*, 1997; Liu and Delcour, 1998a), the activity is modified in isogenic strains that differ only by an engineered mutation at a single site in OmpC. We purposefully did not purify OmpC because purification and reconstitution procedures can affect porin behavior (Lakey and Pattus, 1989; Saxena *et al.*, 1989; Buehler *et al.*, 1991). The traces of wild-type channels, as shown in the figures, appear different from those typically reported in planar lipid bilayers studies, because they are recorded at low voltages where no voltage-dependent inactivation occurs. Thus, transitions of large amplitude due to the simultaneous closures of multiple monomers are rarely seen. However, smaller and faster transitions, usually masked in traces obtained from black lipid membranes, are detected because of the higher filter corner frequency and faster sampling. The amplitudes of the closing transitions have various sizes and typically cluster around values that are integral multiples of the smallest observed value. Because there is no favored conductance level, we made the working hypothesis that the transitions of the smallest amplitude represent a single monomer (rather than a sub-conductance state) and the largest

transitions are those of monomers gating cooperatively, a well-known phenomenon in porins (Delcour *et al.*, 1989b).

For the kinetic analysis of the E109Q mutant, we obtained single-channel current valves from amplitude histograms. Event detection was done by using the half-amplitude criterion and a minimum dwell time of 300 μs (Liu *et al.*, 1997). Relative residence times were calculated as the ratio of total time spent with 0 or 1 or ... *N* channels open to the total time of analyzed data.

Results

Spontaneous gating of wild-type OmpC

Spontaneous transitions between open and closed states of wild-type OmpC porins are readily detected in patch-clamp experiments. Such activity is observed even in the absence of a transmembrane voltage (Liu and Delcour, 1998a) and is distinct from the previously reported voltage-dependent inactivation of porin currents (Schindler and Rosenbusch, 1978; Dargent *et al.*, 1986; Xu *et al.*, 1986; Delcour *et al.*, 1989b; Buehler *et al*, 1991; Berrier *et al.*, 1992). Figure 2 shows a typical recording from a patch containing multiple channels. Despite the use of a reconstitution protocol, the likelihood of obtaining patches with single trimers is extremely low, probably because porins retain their native, highly clustered organization, even in membrane fractions. Since most of the porins channels are open, the current dwells at a non-zero value, typically of the order of 40–100 pA at 60 mV. This macroscopic current gives rise to a baseline level, from which two types of transitions are observed: transient closures of various sizes (upward deflections) and frequent rapid openings (downward deflections). This kinetic signature is clearly distinct from background noise, as evidenced by the comparison with a trace obtained with protein-free liposomes. These transitions originate from the same channel type, because both activities are modified by a single amino acid substitution in OmpC, as shown here and in previous work (Liu *et al.*, 1997; Liu and Delcour, 1998a, 1998b). Although an accurate measurement of gating kinetic parameters cannot be obtained because the activity originates from many channels, we believe that these transitions represent the dynamic interconversion between at least one closed state and two open states. In the rest of the paper, we will use the following terminology to refer to these states: C_1 closures are the transient, often cooperative closures that are seen as upward deflections from the baseline in Figure 2; O_1 openings are the prolonged, favored open state leading to the baseline current level; and O_2 openings are the rapid openings seen as downward deflections from the baseline in Figure 2.

Effect of mutations on L3 and the opposite barrel wall

In order to test whether ionic interactions between L3 and the opposite barrel wall play a role in the spontaneous gating activity of porins, we studied the electrophysiological behavior of either spontaneous or site-directed mutants where a single charged amino acid residue has been replaced by a neutral one.

Figures 2 and 3 show that the D105Q, E109Q and K16Q mutations have altered the gating pattern of OmpC porin in distinct ways, whereas the R124Q substitution left the kinetics of the channel unchanged. The most drastic change is found with E109Q. The channel activity appears homogeneous and the two gating patterns of C_1 closures and O_2 openings are no longer readily recognized. Dwell times at each current level are longer than in wild-type yielding well-resolved transitions.

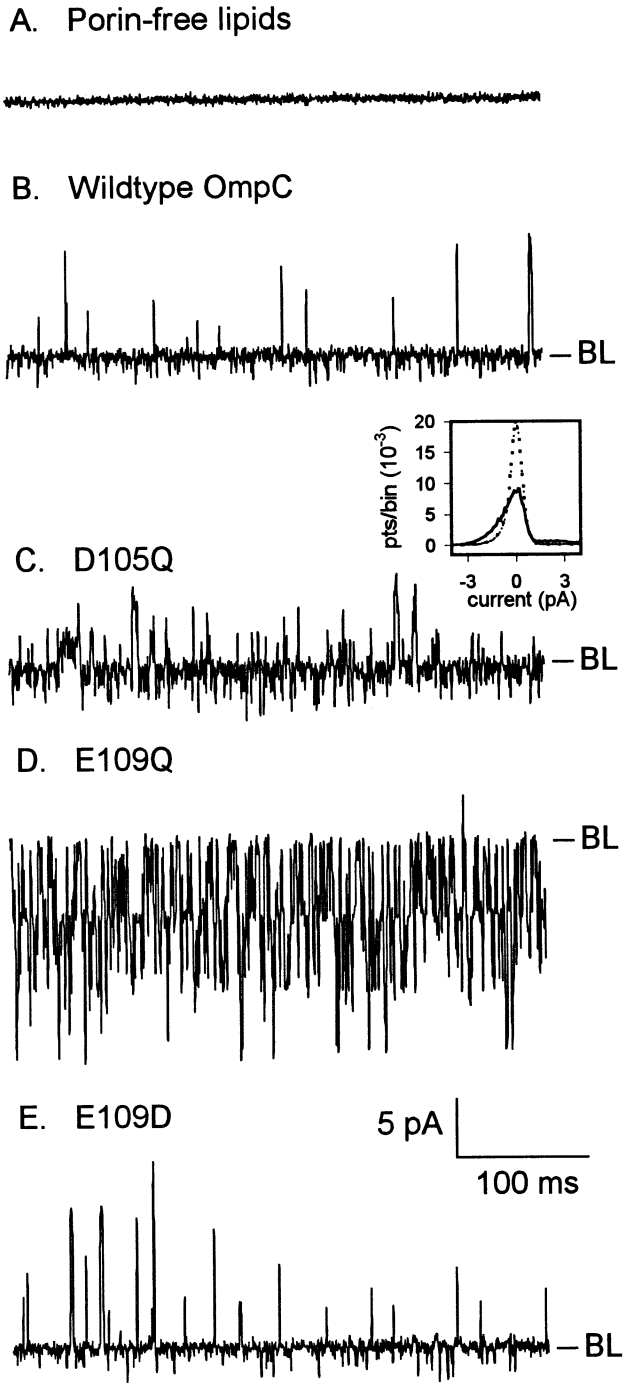

Fig. 2. Representative current traces obtained from porin-free liposomes (**A**) or patches containing wild-type OmpC (**B**) or OmpC porin mutated on the L3 loop, as indicated (**C–E**). The baseline (BL) represents the current passing through all predominantly open porins in the patch. Upward deflections are closures. The pipet voltage was –60 mV. The inset between traces B and C represents the superimposed amplitude histograms obtained from the wild-type trace B (dotted line) and the mutant trace C (solid line). For the sake of comparison, the baseline currents have been arbitrarily set to 0 pA, but they were originally 63 pA for trace B and 75 pA for trace C, testifying that the two patches contain approximately the same number of open pores (~40).

Previous work showed that the activity of E109Q channels is greatly decreased at acidic pH, in a manner similar to the suppression of the O_2 openings of wild-type channels in such conditions (Liu and Delcour, 1998b). We therefore propose that the intense activity of the E109Q mutants stems from an

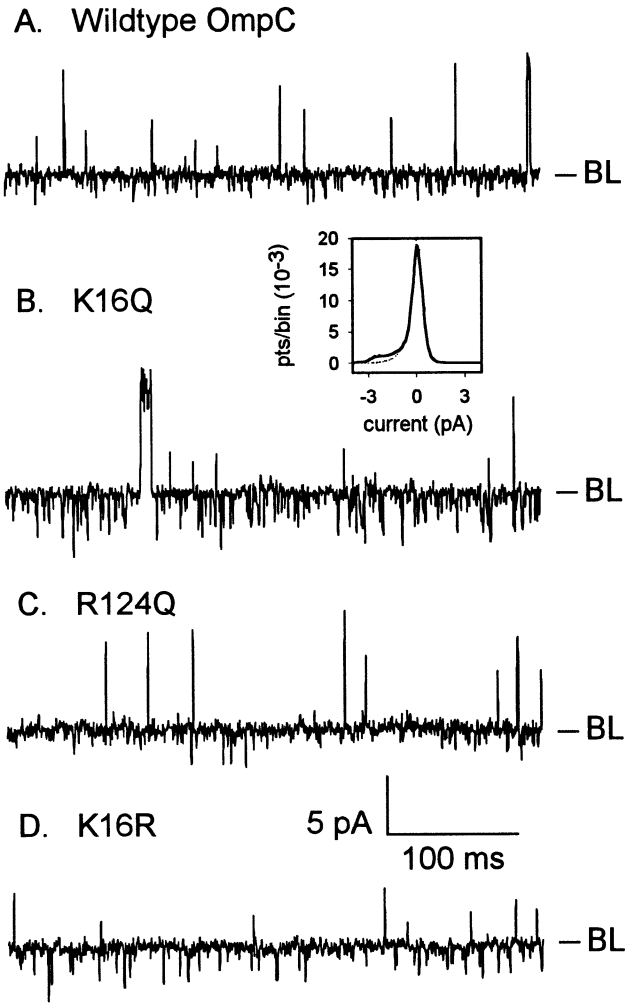

Fig. 3. Representative current traces from patches containing wild-type OmpC (**A**) or site-directed mutants in the barrel, as indicated (**B-D**). The baseline (BL) represents the current passing through all predominantly open porins in the patch. Upward deflections are closures. The pipet voltage was –60 mV. The inset between traces A and B represents the superimposed amplitude histograms obtained from the wild-type trace A (dotted line) and the mutant trace B (solid line). For the sake of comparison, the baseline currents have been arbitrarily set to 0 pA, but they were originally 63 pA for trace A and 61 pA for trace B, testifying that the two patches contain approximately the same number of open pores.

increase in the probability of O_2 openings. Additional evidence for this interpretation will be shown below in the effect of KCl concentration on wild-type and mutant channels. The current fluctuations of E109Q channels display the staircase appearance that characterize the gating of independent channels. This is in sharp contrast to the typical cooperative behavior seen in porin activity (Xu *et al.*, 1986; Delcour *et al.*, 1989b; Berrier *et al.*, 1992). The gating kinetics of the E109Q channels have been observed consistently in more than 20 experiments.

The D105Q and K16Q mutants are also characterized by an increase in the frequency of O_2 openings, but have an overall signature that is closer to wild-type, with an identifiable baseline current level and no effect of the kinetics of the C_1 closures (Figures 2 and 3). These gating patterns were observed reproducibly in over 15 experiments for each mutant. Because the opening transitions are so fast, they cannot be analyzed as individual events on the basis of the event detection criterion typically used for kinetic analysis (see Materials and methods). However, we can use amplitude histograms to demonstrate the increased opening frequency of the mutants relative to wild-type. The amplitude histograms in the insets in Figures 2 and 3 were constructed by arbitrarily assigning a value of 0 pA to the baseline level and negative (or positive) current values to additional openings (or closures) originating from the baseline. In this way, we can overlay histograms obtained from different patches for comparative purposes and eliminate differences in macroscopic current (values are given in the figure captions). The histograms show that the great majority of current values are at the baseline level and that opening and closing transitions of wild-type channels are too infrequent to form additional histogram peaks. However, the increased opening frequency of the mutant channels led to a broadening of the left shoulder of the 0 pA level peak. This can be documented quantitatively by comparing the abscissa of points that have the same ordinate value (e.g. 500 points per bin) and are taken from the two curves. We call this the I_{500} parameter (for current I at the 500-point mark). An increase in the absolute value of this parameter indicates an increase in the frequency of the transient openings. For the amplitude histograms of Figures 2 and 3, the I_{500} parameter shifted from the wild-type value of –1.7 to –2.7 and –3.0 for the D105Q and K16Q mutants, respectively. In the case of the K16Q mutant (Figure 3), the 0 pA peak is completely overlaid over the wild-type histogram. In the case of the D105Q mutant (Figure 2), the 0 pA peak is reduced because of the increase in the percentage of time that the current dwells at non-baseline levels (increase in closing and opening transition frequencies).

The enhanced frequency of O_2 openings in three out four of the mutants suggests that this transition might be governed by ionic interactions between these residues. This interpretation is supported by the lack of effect of conservative substitutions at E109 and K16. As shown in traces E in Figure 2 and D in Figure 3, the patterns of O_2 openings of E109D and K16R are essentially identical with wild-type.

For the investigation of mutations at other positively charged residues of the barrel, we used some of the OmpC mutants isolated and characterized by Misra and Benson (1988). Figure 4 shows traces obtained from patches made on wild-type or mutant channels and having roughly the same macroscopic current (~50 pA at –60 mV). The gating activity of the R37H and R74S mutant channels is essentially identical with that of wild-type OmpC in the parent strain. A double mutant (R37H/R74S), however, shows an enhanced activity at the baseline level. These fast transitions become much reduced when the pH of the bath solution is decreased to 5.4 (Figure 4E). This sensitivity to pH, which is a hallmark of O_2 openings in wild-type and K16Q (Liu and Delcour, 1998b), suggests that these fast transitions represent O_2 openings whose frequency is increased in this mutant.

We did not focus our attention on the study of voltage sensitivity of these mutants, since this has been essentially accomplished by others on OmpC (Lakey *et al.*, 1991) and on homologous mutants in OmpF and PhoE (Saint *et al.*, 1996; Van Gelder *et al.*, 1997a). In accordance with the published results, we found that the mutations that eliminate charges on the L3 loop (D105Q, E109Q) have reduced voltage sensitivity, whereas mutations that reduce charges on the opposite barrel wall (K16Q, R124Q) have enhanced voltage sensitivity (data not shown).

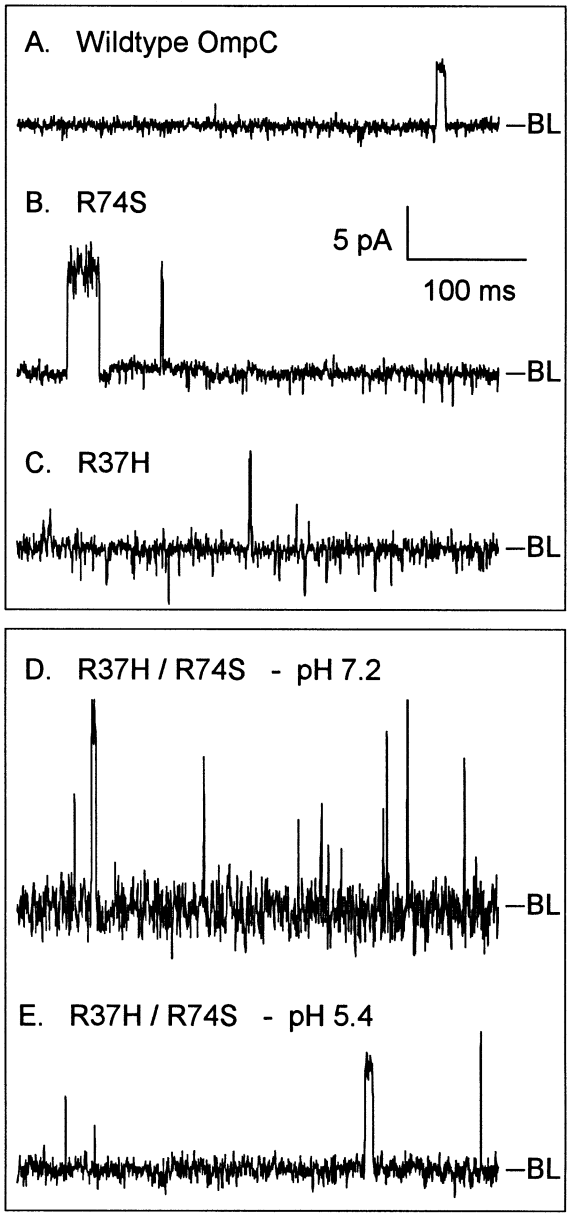

Fig. 4. Representative current traces from patches containing wild-type OmpC from strain RAM105 (**A**) or spontaneous mutants in the barrel from strain RAM120 (**B**), RAM272 (**C**) and RAM359 (**D** and **E**). Traces D and E were obtained at the indicated bath pHs (pipet pH was 7.2). Note the drastic reduction of gating activity at acidic pH. The baseline (BL) represents the current passing through all predominantly open porins in the patch. Upward deflections are closures. The pipet voltage was –60 mV.

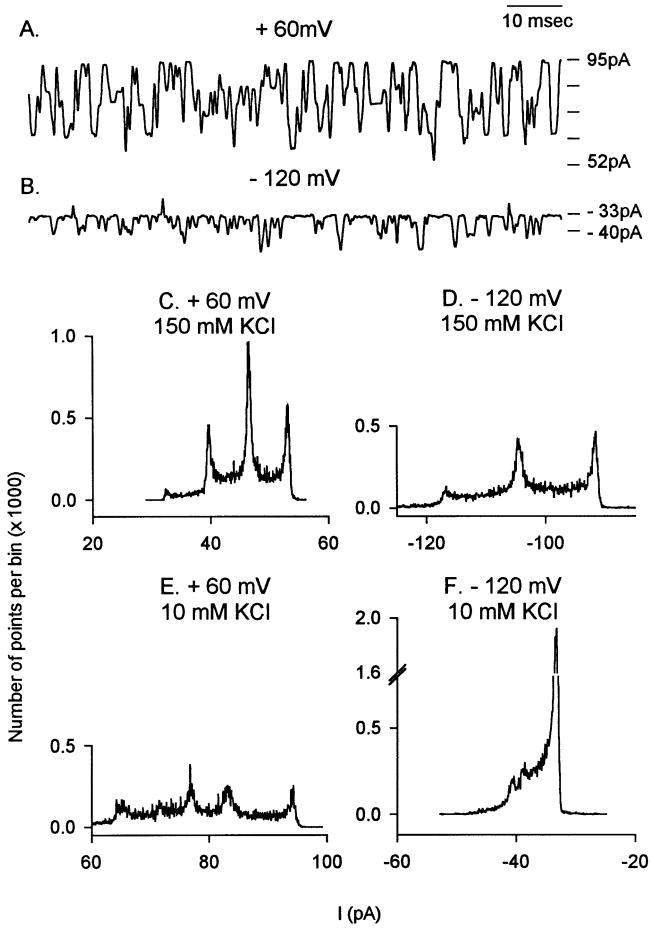

Fig. 5. Lowering the concentration of permeant ions affects gating activity of the E109Q mutant. (**A** and **B**) Current recordings were obtained from the same patch of E109Q mutant channels at the indicated pipet potentials in 5 mM HEPES, 0.1 mM K-EDTA, 10 μM $CaCl_2$, pH 7.2, containing 150 mM KCl in the pipet solution and 10 mM KCl in the bath solution. Values of the total current through the patch are indicated at the right of the traces. Tick marks represent the current levels corresponding to the opening of successive monomers (single channel amplitudes are 10.7 pA at +60 mV and 7 pA at –120 mV). Channel openings are represented by upward deflections at +60 mV and downward deflections at –120 mV. (**C**–**F**) Amplitude histograms were generated from 10 s long recordings from a single experiment on E109Q mutant channels. The pipet voltages were as indicated. Bin was 0.1 pA. The KCl concentration in the pipet was 150 mM and in the bath as indicated. Peak values are as follows (in pA): 32.4, 39.6, 46.4 and 52.9 (panel C); –126.4, –116.7, –104.3 and –91.6 (panel D); 65.1, 76.6, 83.0 and 93.9 (panel E); –39.6 and –33.2 (panel F).

Effect of permeant ion concentration on mutant and wild-type channels

The data collected from the mutants suggest that ionic interactions between L3 and the opposite barrel wall may play a role in the spontaneous gating of porin, in particular in the pattern of O_2 openings. If this is correct, a disruption in the kinetics of open-closed transitions would be expected when the ionic strength of the solution filling the pore is changed, because of the greater shielding of the electric field at higher ionic strength. In order to test this hypothesis, we recorded the activity of OmpC channels in different concentrations of KCl. In order to make comparisons in the same patch, we left the pipet concentration constant at 150 mM KCl and recorded the channel activity sequentially in symmetric and then asymmetric conditions, with a bath concentration of either 10 mM or 1 M KCl. We first did these experiments with the E109Q mutant, reasoning that the enhanced gating activity of the O_2 transitions in this mutant would facilitate the detection of any effect. Although the electrostatic interactions across the eyelet of E109Q channels are weakened by the mutation, we found that the channels are still sensitive to changes in ion concentration.

Figure 5A and B show the activity of the E109Q channels in asymmetric conditions (150 mM KCl in the pipet; 10 mM KCl in the bath), at the indicated pipet voltages. In these asymmetric conditions, the observed reversal potential is ~ –55 mV (pipet voltage) and we had to use a pipet voltage more negative than –60 mV to obtain detectable current amplitudes. Thus, we compared the gating activity in symmetric and asymmetric conditions at +60 and –120 mV. At positive

pipet potentials, when the current is predominantly carried by K^+ ions leaving the pipet, the gating of the channel is identical with that in symmetric 150 mM KCl (compare the staircase-like activity in Figures 2D and 5A, but note the different time scales). At pipet potentials more negative than E_K, when K^+ ions are moving inside the pipet from the low ionic strength bath solution, the channel kinetics are greatly affected. The probability of O_2 openings is much reduced and a preferred baseline level is observed (at –33 pA in Figure 5B).

To document this effect further, we generated amplitude histograms for the E109Q mutant channels in four conditions applied to the same patch (Figure 5C–F). In all cases, the pipet solution contained 150 mM KCl and the concentration of KCl in the bath is as indicated in the panels. In symmetric conditions (panels C and D), the current amplitudes distribute among four levels of conductance (see caption for peak current values), representing the gating of three independent channels (presumably monomers). The relative area under these peaks is representative of the amount of time spent at each level. For example, at positive pipet voltage (Figure 5C), the peak at the lowest conductance value (~32.4 pA) is also the smallest, indicating a low probability of all three channels being closed. In asymmetric conditions, a drastic modification in the shape of the amplitude histograms occurs, but only at negative pipet potentials, i.e. when the current is carried by K^+ ions leaving the 10 mM KCl containing bath solution (Figure 5F). This lopsided amplitude histogram arises from the change in opening probability: when the concentration of the permeant ion is low, the majority of the channels are closed and the predominant peak becomes that of lowest current amplitude (–33.2 pA in Figure 5F).

We also performed experiments in which the KCl concentration of the bath was raised. Figure 6A and B show that the shape of amplitude histograms of E109Q channels changes when the bath solution is switched from 150 mM to 1 M KCl. In 150 mM KCl (Figure 6A), the peak at the lowest current amplitude (–41.5 pA) is taller than that at the highest current amplitude (–60.5 pA), as expected for channels that are rarely open simultaneously. In 1 M KCl (Figure 6B), the relationship between the relative heights of the peaks of lowest (–62.7 pA) and highest (–97.7 pA) amplitude is reversed and the current dwells more frequently at the –97.7 pA level than at the –62.7 pA level. This illustrates that the probability of finding all channels simultaneously open is increased (current values and distances between peaks are larger than in Figure 6A because of the increased concentration of permeant ions).

We can also document this effect by measuring the relative percentage of time for which the current dwells at levels corresponding to 0, 1, ... *N* open channels. The results obtained from two patches, one containing three actively gating channels (Figure 6C) and the other nine such channels (Figure 6D), illustrate that there is a shift in the distribution of the relative residence times. In 1 M KCl (closed symbols), more channels spend a larger fraction of the time in the open state than in 150 mM KCl (open symbols). This trend was observed in five experiments, where there was an average 1.37-fold increase (significant at $p < 0.01$, paired *t*-test) in the open probabilities when the bath solution was switched from 150 mM to 1 M KCl.

These effects are also observed with wild-type channels. Because of the already low probability of O_2 openings in wild-type channels, the inhibitory effect of low ionic strength buffer is barely detectable (Figure 7A and B). Only a slight decrease in the occurrence of openings from the baseline level (downward

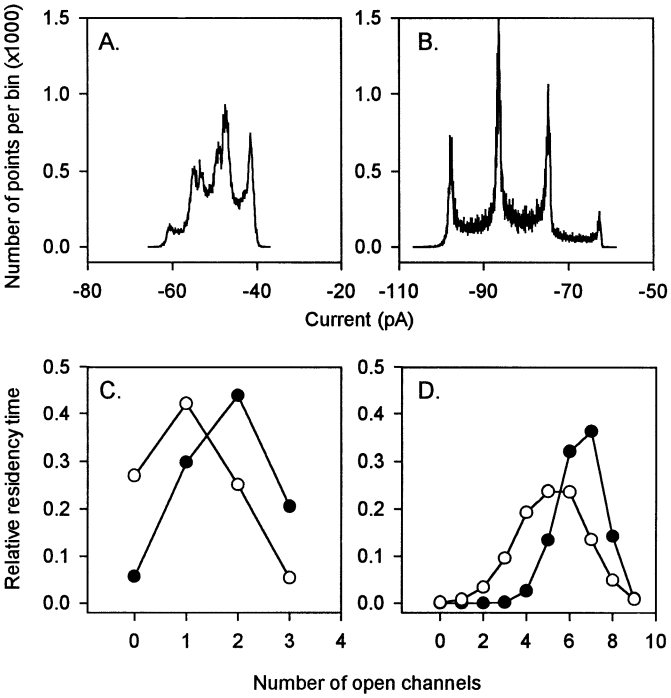

Fig. 6. Increasing the permeant ion concentration affects gating activity of the E109Q mutant. (**A** and **B**) Amplitude histograms were generated from 8.2 s long recordings from a single experiment on E109Q mutant channels. The bath solution contained 5 mM HEPES, 0.1 mM K-EDTA, 10 μM $CaCl_2$, pH 7.2 with either 150 mM KCl (A) or 1 M KCl (B). In both cases, the pipet solution contained 150 mM KCl and the pipet voltage was –60 mV. Note the relative change in peak amplitudes upon buffer change. (**C** and **D**) The calculation of the relative residence times is given in Materials and methods. Open symbols, 150 mM KCl; closed symbols, 1 M KCl, in the bath solution. The pipet solution contained 150 mM KCl and the pipet voltage was –60 mV (C) and –30 mV (D).

deflections) is observed. However, increasing the KCl concentration in the bath has clearly promoted openings from the baseline level (Figure 7C and D). These observation are in agreement with the results from the E109Q mutant. It is noteworthy that the kinetics of closures from the baseline level (O1 → C1 transitions, upward deflections) remains completely unaffected by the manipulations of KCl concentrations. A selective effect of permeant ion concentration on O_2 openings but not C_1 closures has been consistently observed in other mutants where it was tested, such as D105Q, E109D, K16R, D315A, D118Q and R92Q (the last three were described in a previous publication; Liu and Delcour, 1998a). Similar experiments on K16Q and R124Q could not be performed unambiguously because of the enhanced voltage dependence of the C1 closures in these mutants.

Discussion

General diffusion porins, such as OmpC, OmpF or PhoE, are usually thought to behave as rigid pores, that solely confer molecular sieving properties to the outer membrane of *E.coli*. A voltage-dependent inactivation has been evidenced by many groups (Schindler and Rosenbusch, 1978; Dargent *et al.*, 1986; Delcour *et al.*, 1989b; Berrier *et al.*, 1992), but because of the apparently high voltages required (Xu *et al.*, 1986; Buehler *et al.*, 1991; Saint *et al*, 1996, although also see Delcour *et al.*, 1989b; Iyer and Delcour, 1997; Samartzidou and Delcour, 1998), it is not yet clear that this dynamic property is physiologically relevant. In recent years, we and others (Berrier

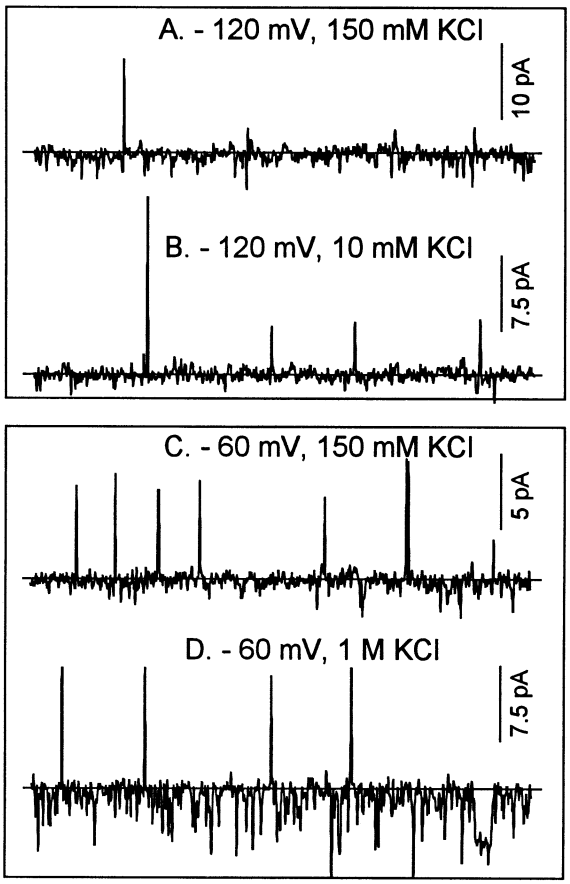

Fig. 7. Permeant ion concentration influences the probability of O_2 openings in wild-type OmpC. Representative 200 ms long current recordings obtained from the same patch are shown in bath solutions containing the indicated KCl concentrations. In all cases, pipet solutions were 150 mM KCl. Pipet voltages were –120 mV (**A** and **B**) or –60 mV (**C** and **D**). Different scales are used for the ordinate to keep comparable sizes of single channel transitions, despite changes in single channel current values upon buffer changes. The baseline level is represented as a horizontal line through the traces. Upward transitions are closures.

et al., 1992; Saint *et al.*, 1993) have demonstrated that, in addition to voltage-dependent inactivation, porins undergo spontaneous transitions between closed and open states. This behavior is highly cooperative and modulated by a variety of parameters, including transmembrane voltage (Delcour *et al.*, 1989b; delaVega and Delcour, 1995; Iyer and Delcour, 1997; Liu and Delcour, 1997; Samartzidou and Delcour, 1998). Although we have been unable to characterize rigorously this gating activity (which would require the analysis of a single channel or pore-forming subunit and is not possible with these trimeric porins), the study of mutants and of modulation of wild-type channels has allowed us to propose that at least one closed state and two open states are visited during the spontaneous activity (Liu *et al.*, 1997).

In order to understand the molecular basis for this dynamic aspect of porin activity, we engineered several site-directed mutants, targeting the L3 loop and the barrel wall at the constriction zone. It appears that the multiple kinetic states of OmpC porins are governed by different types of interactions. We showed previously that transitions between the closed state and the highly cooperative open state (O_1) were governed by interactions between the L3 loop and the barrel wall. In particular, a hydrogen bond network between the tip of L3 and the adjacent barrel wall and a salt bridge at the root of L3 were implicated (Liu and Delcour, 1998a). Here we studied a different group of residues, namely charged residues that are believed to participate in the formation of an intrinsic electrical field at the constriction zone. They consist of two negatively charged amino acids located on L3 (D105 and E109) and a cluster of positively charged residues on the opposite barrel wall (K16, R37, R74 and R124). Taken all together, the results suggest that electrostatic interactions at the eyelet do not influence the C_1 closures, but affect the kinetics of O_2 openings. Because the patches contain multiple channels, we cannot tell whether the O_2 openings represent transitions from a completely closed (non-ion-conducting) state or transitions from an already open pore to a conformation allowing a higher conductance. In any case, the conformational change that underlies these functional states appears to involve some of the charged residues that surround the eyelet of the OmpC channel.

Not all mutations led to changes in gating pattern. For example, the R37H, R74S and R124Q mutants were without effect. However, the combination of two ineffective mutations (R37H and R74S) induced a gating kinetics that is distinct from wild-type. On the other hand, the charge removal conferred by the mutations at the D105, E109 and K16 residues is effective at bringing a kinetic change. Interestingly, these three residues, in particular E109 and K16, are relatively close to each other in the three-dimensional structure and therefore likely to interact strongly with each other. Such an interaction may not be as strong between the arginines of the barrel cluster and the negatively charged residues of the L3 loop, because these two groups of residues are separated by several ångströms of an aqueous medium filled with permeant ions. Thus, for the arginine cluster, only a dual charge removal might be required to alter the electrostatic interactions with L3 sufficiently to produce an effect on gating. Interestingly, we found that, when calculated from the K16, R37, D105 and E109 residues, the dipole moment drops from 61 D in wild-type to 43 D in the R37H/R74S double mutant, but stays essentially identical in the R37H mutant (63 D) or less affected in R74S mutant (55 D). These values are larger than those found in the most affected mutants K16Q (49 D), D105Q (40 D) and E109Q (50 D).

Since electrostatic interactions are dependent on charge and distance, it can be inferred that the relative positions and ionization states of the residues K16, D105 and E109, may play a key role in controlling the channel opening and closing kinetics. The channels also show a greater ability to undergo the transitions to the O_2 state when the concentration of permeant ions filling the pore is high. Presumably, the high ionic concentration within the pore during permeation provides a greater shielding effect on the electrostatic interactions across the constriction zone. The ensuing weaker attractive interaction of the L3 loop with the barrel in turn results in stabilizing the O_2 state.

What is the origin of the spontaneous transitions to the O_2 state in wild-type? One interpretation is that in wild-type at normal ionic strength, fluctuations in the ionic interactions between the L3 loop and the opposite barrel wall result from subtle conformational changes in L3, possibly a small movement away from the opposite barrel or a breathing of the two segments of the loop. Although the crystal structure of OmpF hints at a fairly rigid L3 loop, it would be naive to picture the protein as a perfectly motionless body once in its native environment. We envision that thermal fluctuations or possibly electrostatic oscillations linked to permeation might

trigger small conformational changes that give rise to the O_2 state. Two possibilities exist: either the channel opens from a closed state into the O_2 state or the O_2 state originates from the O_1 state. We favor this second interpretation since it is likely to require less drastic protein motions. In this case, the O_2 state might simply represent a wider pore or a pore whose charge configuration provides less of an electrostatic barrier to ion flux. The weakening of the electrostatic interactions in the mutants or in the presence of high ionic strength solution would allow for a more favorable distancing of L3 from the opposite barrel wall and thus an increased frequency of the O_2 transitions. In other words, based on the observation that the mutants are more likely to reach the O_2 open state than wild-type, we infer that electrostatic changes can lead to enhanced transitions to the O_2 state. These transitions may not require large conformational changes.

This interpretation of the mutant behavior is based on the assumption that the mutations have not induced a drastic change in the pore conformation. This would need to be confirmed by extensive molecular dynamics simulations of all the mutant structures, which are beyond the scope of the present study. If large conformational changes had been introduced by the mutations, the interpretation of the data might be more difficult. However, it is worth mentioning that, except for E109Q, all other mutants display kinetics of cooperative closures and conductance values that are similar to wild-type. Hence it is likely that the pore structure has not been profoundly altered in those mutants. The E to Q mutation at residue 109 introduced an unexpected and peculiar behavior, namely the loss of cooperative behavior. This is very interesting, considering the fact that this residue is entirely pore-exposed and does not make any direct or indirect contact with other subunits. The E109Q mutant is, therefore, one of the prime candidates for more extensive modeling. Although speculative, the proposed mechanism that electrostatic interactions between pore residues play a role in gating remains at present a viable model considering the effects of manipulating the ionic strength and the selective effect of the mutations on the kinetics of openings, but not closures.

It is not unlikely that spontaneous fluctuations in electrostatic interactions at the eyelet occur during permeation, as the passing ions interact with the channel protein. The X-ray structure shows a constriction zone of 7×10 Å and porins are often described as water-permeable pores allowing ion diffusion as in solution. However, we have evidence that interactions do occur between the fluxing ions and the pore, because rectification of current through single monomers is observed when the permeant ion is switched from potassium to sodium or lithium (Delcour *et al.*, 1989b). Here we suggest that such interactions of the ions during their passage in the pore can promote the channel to visit transiently distinct functional states. Permeation and gating of ion channels are traditionally considered as separate phenomena. Earlier work had already challenged this view (Swenson and Armstrong, 1981). However, recent years have seen the appearance of more and more compelling examples, such as the proposal that a collapse of the pore at the selectivity filter occurs upon the slow (C-type) inactivation of K^+ channels (Liu *et al.*, 1996). Effects of permeant ions on fast gating processes have also been demonstrated in various channel types (Pusch *et al.*, 1995; Chen and Miller, 1996; Townsend and Horn, 1999) and mutations at the pore region of K^+ or Na^+ channels have been documented to stabilize the open state (Tomaselli *et al.*, 1995; Zheng and Sigworth, 1997). Although the pore of these oligomeric channels is most likely made at the subunit interfaces (Chang *et al.*, 1998; Doyle *et al.*, 1998), it is likely that the underlying principle that permeating ions can have a direct influence on the thermodynamic stability of channel conformations applies to all channels, whether they are based on α-helical or β-barrel motifs.

Acknowledgements

We gratefully acknowledge Spencer Benson for the RAM strains and Tilman Schirmer for providing the pdb coordinates of OmpK36 prior to publication. We thank Daniel T.Colbert for insightful and valuable discussions. Thanks are due to Linda Guynn for DNA sequencing and Ramkumar Iyer for reading the manuscript. This work was supported by grants from the NIH (AI34905 to A.H.D. and GM56553 to J.M.B.) and an Award from the Oak Ridge Associated Universities (J.M.B.).

References

Alberti,S., Rodriquez-Quinones,F., Schirmer,T., Rummel,G., Tomas,J.M., Rosenbusch,J.P. and Benedi,V.J. (1995) *Infect. Immun.*, **63**, 903–910.
Antosiewicz,J., Briggs,J.M., Elcock,A.H., Gilson,M.K. and McCammon,J.A. (1996) *J. Comput. Chem.*, **17**, 1633–1644.
Bainbridge,G., Mobasheri,H., Armstrong,G.A., Lea,E.J.A. and Lakey,J.H. (1998) *J. Mol. Biol.*, **275**, 171–176.
Bauer,K., Stuyvé,M., Bosch,D., Benz,R. and Tommassen,J. (1989) *J. Biol. Chem.*, **264**, 16393–16398.
Benson,S.A., Occi,J.L.L. and Sampson,B.A. (1988) *J. Mol. Biol.*, **203**, 961–970.
Berrier,C., Coulombe,A., Houssin,C. and Ghazi,A. (1992) *FEBS Lett.*, **306**, 251–256.
Berrier,C., Besnard,M.and Ghazi,A. (1997) *J. Membr. Biol.*, **156**, 105–115.
Buehler,L.K., Kusumoto,S., Zhang,H. and Rosenbusch,J.P. (1991) *J. Biol. Chem.* **266**, 24446–24450.
Chang,G., Spencer,R.H., Lee,A.T., Barclay,M.T. and Rees,D.C. (1998) *Science* **282**, 2220–2226.
Chen,T.Y. and Miller,C. (1996) *J. Gen. Physiol.*, **108**, 237–250.
Cowan,S.W., Schirmer,T., Rummel,G., Steiert,M., Ghosh,R., Pauptit,R.A., Jansonius,J.N. and Rosenbusch,J.P. (1992) *Nature*, **358**, 727–733.
Dauber-Osguthorpe,P., Roberts,P.V.A., Osguthorpe,D.J., Wolff,J., Genest,M. and Hagler,A.T. (1988) *Proteins: Struct. Funct. Genet.,* **4,** 31–47.
Dargent,B., Hofmann,W., Pattus,F. and Rosenbusch,J.P. (1986) *EMBO J.*, **5**, 773–778.
delaVega,A.L. and Delcour,A.H. (1995) *EMBO J.*, **14**, 6058–6065.
Delcour,A.H. (1997) *FEMS Microbiol. Lett.*, **151**, 115–123.
Delcour,A.H., Martinac,B., Kung,C. and Adler,J. (1989a) *Biophys. J.*, **56**, 631–636.
Delcour,A.H., Martinac,B., Kung,C. and Adler,J. (1989b) *J. Membr. Biol.*, **112**, 267–275.
Delcour,A.H., Adler,J.and Kung,C. (1991) *J. Membr. Biol.*, **119**, 267–275.
Delcour,A.H., Kung,C., Adler,J. and Martinac,B. (1992) *FEBS Lett.*, **304**, 216–220.
Doyle,D.A., Cabral,J.M., Pfuetzner,R.A., Kuo,A., Gulbis,J.M., Cohem,S.L., Chait,B.T. and MacKinnon,R. (1998) *Science*, **280**, 69–77.
Dutzler,R., Rummel,G., Alberti,S., Hernaandez-Allés,S., Phale,P.S., Rosenbusch,J.P., Benedi,V.J. and Schirmer,T. (1999) *Structure*, **7**, 425–434.
Eppens,E.F., Saint,N., Van Gelder,P., van Boxtel,R. and Tommassen,J. (1997) *FEBS Lett.*, **415**, 317–320.
Fogolari,F., Esposito,G., Viglino,P., Briggs,J.M. and McCammon,J.A. (1998) *J. Am. Chem. Soc.*, **120**, 3735–3738.
Gilson,M. and Honig,B. (1988) *Proteins,* **4,** 7–18.
Hamill,O.P., Marty,A., Neher,E., Sakmann,B. and Sigworth,F.J. (1981) *Pflügers Arch.*, **391**, 85–100.
Ingham,C., Buechner,M. and Adler,J. (1990) *J. Bacteriol.*, **172**, 3577–3583.
Iyer,R. and Delcour,A.H. (1997) *J. Biol. Chem.*, **272**, 18595–18601.
Karshikoff,A., Spassov,V., Cowan,S.A., Ladenstein,R.and Schirmer,T. (1994) *J. Mol. Biol.*, **240**, 372–377.
Kraulis,P.J. (1991) *J. Appl. Crystallogr.*, **24**, 946–950.
Lakey,J.H. (1987) *FEBS Lett.*, **211**, 1–4.
Lakey,J.H. and Pattus,F. (1989) *Eur. J. Biochem.*, **186**, 303–308.
Lakey,J.H., Lea,E.J.A. and Pattus,F. (1991) *FEBS Lett.*, **278**, 31–34.
Liu,N. and Delcour,A.H. (1998a) *Protein Eng.*, **11**, 797–802.
Liu,N. and Delcour,A.H. (1998b) *FEBS Lett.*, **434**, 160–164.
Liu,N., Benedik,M.J. and Delcour,A.H. (1997) *Biochim. Biophys. Acta*, **1326**, 201–212.

Liu,Y., Jurman,M.E.and Yellen,G. (1996) *Neuron*, **16**, 859–867.
Madura,J.D. *et al.* (1995) *Comput. Phys. Commun.*, **91**, 57–95.
Misra,R. and Benson,S.A. (1988) *J. Bacteriol*., **170**, 3611–3617.
Mizuno,T., Chou,M.-Y. and Inouye,M. (1983) *J. Biol. Chem*., **258**, 6932–6940.
Nikaido,H. (1996) In Neidhardt,F.C. (ed.), *Escherichia coli and Salmonella. Cellular and Molecular Biology.* ASM Press, Washington, DC, pp. 29–47.
Nicholls,A., Sharp,K. and Honig,B. (1991) *Proteins: Struct. Funct. Genet.*, **11**, 281–296.
Pautsch,A. and Schulz,G.E. (1998) *Nature Struct. Biol.*, **5**, 1013–1017.
Phale,P.S., Schirmer,T., Prilipov,A., Lou,K.-L., Hardmeyer,A. and Rosenbusch,J.P. (1997) *Proc. Natl Acad. Sci. USA*, **94**, 6741–6745.
Pusch,M., Ludewig,U., Rehfeldt,A.and Jentsch,T.J. (1995) *Nature*, **373**, 527–531.
Saint,N., De,E., Julien,S., Orange,N. and Molle,G. (1993) *Biochim. Biophys. Acta*, **1145**, 119–123.
Saint,N., Lou,K.-L., Widmer,C., Luckey,M., Schirmer,T. and Rosenbusch,J.P. (1996) *J. Biol. Chem.*, **271**, 20676–20680.
Sali,A. and Blundell,T.L. (1993) *J. Mol. Biol.,* **234,** 779–815.
Sali,A., Pottertone,L., Yuan,F., van Vlijmen,H. and Karplus,M. (1995) *Proteins,* **23,** 318–326.
Samartzidou,H. and Delcour,A.H. (1998) *EMBO J.*, **17**, 93–100.
Saxena,R.K., Ishii,J.and Nakae,T. (1989) *Curr. Microbiol*,. **19**, 189–191.
Schindler,H. and Rosenbusch,J.P. (1978) *Proc. Natl Acad. Sci. USA*, **75**, 3751–3755.
Schirmer,T., Keller,T.A., Wang,Y.-F. and Rosenbusch,J.P. (1995) *Science*, **267**, 512–514.
Schulz,G. E (1996) *Curr. Opin. Struct. Biol.*, **6**, 485–490.
Swenson,R.P.,Jr and Armstrong,C.M. (1981) *Nature*, **291**, 427–429.
Tomaselli,G.F., Chiamvimonvat,N., Nuss,H.B., Balser,J.R., Pérez-Garcìa,M.T., Xu,R.H., Orias,D.W., Backx,P.H. and Marban,E. (1995) *Biophys. J.*, **68**, 1814–1827.
Townsend,C. and Horn,R. (1999) *J. Gen. Physiol*., **113**, 321–332.
Van Gelder,P., Saint,N., Phale,P., Eppens,E.F., Prilipov,A., van Boxtel,R., Rosenbusch,J.P. and Tommassen,J. (1997) *J. Mol. Biol*., **269**, 468–472.
Weiss,M.S., Abele,U., Weckesser,J., Welte,W., Schiltz,E.and Schulz,G.E. (1991) *Science*, **254**, 1627–1630
Xu,G., Shi,B., McGroarty,E.J. and Tien,H.T. (1986) *Biochim. Biophys. Acta*, **862**, 7–64.
Zheng,J. and Sigworth,F.J. (1997) *J. Gen. Physiol*., **110**, 101–117.

Received February 22, 2000; revised April 17, 2000; accepted May 9, 2000